HHS Public Access

Author manuscript

Chem Biol Drug Des. Author manuscript; available in PMC 2016 June 23.

Published in final edited form as:

Chem Biol Drug Des. 2008 March ; 71(3): 205–215. doi:10.1111/j.1747-0285.2008.00628.x.

Antiviral and Anticancer Optimization Studies of the DNA-binding Marine Natural Product Aaptamine

John J. Bowling[1], **Hari K. Pennaka**[1], **Kelly Ivey**[1], **Subagus Wahyuono**[2], **Michelle Kelly**[3], **Raymond F. Schinazi**[4], **Frederick A. Valeriote**[5], **David E. Graves**[6], and **Mark T. Hamann**[7,*]

[1]Department of Pharmacognosy, School of Pharmacy and The University of Mississippi, University, MS 38677, USA [2]Department of Pharmaceutical Biology, Faculty of Pharmacy, Gadjah Mada University, Sekip Utara, Yogyakarta 55281, Indonesia [3]National Centre for Aquatic Biodiversity and Biosecurity, National Institute of Water and Atmospheric Research, Private Bag 109695, Newmarket, Auckland, New Zealand [4]Department of Pediatrics, Center for AIDS Research and Laboratory of Biochemical Pharmacology, Emory University School of Medicine, Atlanta, GA 30332, USA [5]Henry Ford Health System, Department of Internal Medicine, Division of Hematology and Oncology, Detroit, MI 48202, USA [6]Department of Chemistry, University of Alabama at Birmingham, 901 14th Street South, Birmingham, AL 35294, USA [7]Departments of Pharmacognosy, Pharmacology, Chemistry and Biochemistry and The National Center for the Development of Natural Products, The University of Mississippi, University, MS 38677, USA

Abstract

Aaptamine has potent cytotoxicity that may be explained by its ability to intercalate DNA. Aaptamine was evaluated for its ability to bind to DNA to validate DNA binding as the primary mechanism of cytotoxicity. Based on UV–vis absorbance titration data, the K_{obs} for aaptamine was 4.0 (±0.2) × 10^3 which was essentially equivalent to the known DNA intercalator *N*-[2-(diethylamino)ethyl]-9-aminoacridine-4-carboxamide. Semi-synthetic core modifications were performed to improve the general structural diversity of known aaptamine analogs and vary its absorption characteristics. Overall, 26 aaptamine derivatives were synthesized which consisted of a simple homologous range of mono and di-*N*-alkylations as well as some 9-*O*-sulfonylation and bis-*O*-isoaaptamine dimer products. Each product was evaluated for activity in a variety of whole cell and viral assays including a unique solid tumor disk diffusion assay. Details of aaptamine's DNA-binding activity and its derivatives' whole cell and viral assay results are discussed.

*Corresponding author: Mark T. Hamann, mthamann@olemiss.edu.

[C]Log D calculated using calculator plugins for structure property prediction and calculation, MarvinBeans 4.1.2, 2006, ChemAxon (http://www.chemaxon.com/demosite/marvin/index.html).

Supplementary Material

Supplementary material including NCI 60-Cell Panel Cytotoxicity Results for compounds **17, 20, 27, 30** as well as H^1 and C^{13} – NMR Spectra For Compounds **5–30** are available online.

This material is available as part of the online article from: http://www.blackwell-synergy.com/doi/abs/10.1111/j.1747-0285.2007.00628.x

(This link will take you to the article abstract).

Please note: Blackwell Publishing are not responsible for the content or functionality of any supplementary materials supplied by the authors. Any queries (other than missing material) should be directed to the corresponding author for the article.

Keywords

aaptamine; alkaloid; anti-HIV; cytotoxicity; DNA binding; infectious diseases; natural products

Aaptamine (**1**; Figure 1) is commonly isolated in large yields from various species of the marine sponge genus *Aaptos* (Order Hadromerida: Family Suberitidae)[a], along with a handful of related compounds such as isoaaptamine (**2**) which contain the benzonapthyridine core structure (1–7). The isolation of aaptamine from the taxonomically unrelated species *Luffariella* (Order Dictyoceratida: Family Thorectidae) (3), *Hymeniacidon* (Order Halichondrida: Family Halichondriidae) (6), and *Xestospongia* (7) (Order Haplosclerida: Family Petrosiidae)[b], indicates the likelihood of production of aaptamine from a microbial source. In fact, several novel metabolites containing the aaptamine core have come from one particular sponge (7), underlining likely contributions of the microbial community associated with the producer of aaptamine. A number of total synthetic studies have been published along with a limited collection of semi-synthetic derivatives since its original discovery (8–16). Considering its low molecular weight, aaptamine is relatively difficult to synthesize from available starting materials. Attempts to complete the unique fused tricycle have been made through quinoline and isoquinoline precursors, the best overall yield being 13 percent over 14 steps. Although the synthetic yield is low, it is likely to be the more cost efficient choice for the production of aaptamine, unless a microbial producer is found.

The proposed biogenesis of aaptamine suggests a possible Pictet-Spengler type condensation commonly attributed to many other natural alkaloids (16). Likewise, three common pharmacophores can be recognized in the aaptamine scaffold: isoquinoline, the largest class of alkaloids isolated from medicinal plants; dopamine, a compound affecting the central nervous system and behavior; and finally, quinoline, known primarily for its anti-malarial properties.

Aaptamine's potential for drug development is further evidenced by the actual results of a highly diverse group of molecular targets already evaluated. In addition to antiviral (5,17) and anticancer (4,6,18) activities, the aaptamines have a strong in vitro radical scavenging capacity (19) and have been shown to block α-adrenoceptor action (1) as well as inhibit α-1,3-glucanase (20) and monoamine oxidase (21). Still, compounds which are active against a variety of targets are certain to encounter problems with indiscriminant toxicities. It is important to recognize toxicity as a hurdle for the development of aaptamine as a useful drug but not let it prohibit the evaluation of its derivatives for therapeutic potential. The ‘privileged structures’ approach (22) is dependent on exploiting a scaffold's common

[a]A variety of species of *Aaptos* have been named in the production of aaptamine above, including sponges identified as *Aaptos aaptos* (1,2,4) or simply *Aaptos* sp. (5). Kelly-Borges and Bergquist (33) indicated that it was highly unlikely that *Aaptos aaptos* (Schmidt, 1864), originally described from Lagoste, Algeria, was ‘cosmopolitan’ as much of the earlier literature suggested, but that specimens from locations such as Okinawa (1,2) might be closer to *Aaptos niger* Hoshino. Similarly, the specimens described as ‘*Aaptos* sp.’ (5) from Brazil, is most likely either *A. nigra* Lévi (blackish dark orange to gold with a deep yellow interior), or *A. chromis* de Laubenfels, 1954 (bright green with a yellow interior).

[b]A re-examination of the specimen in Calcul *et al.* (2003) has confirmed that the sponge is most closely related to the widely spread Indo-Pacific sponge *Neopetrosia exigua* (Kirkpatrick, 1900) (Order Haplosclerida: Family Petrosiidae), formerly known as *Xestospongia exigua*. The genus *Neopetrosia* is clearly phylogenetically distinct from the genus *Aaptos* (Order Hadromerida: Family Suberitidae).

mechanism of drug-target interaction for multiple targets. In a similar fashion, a key for the development of the aaptamine scaffold is the identification of its common mechanism of drug-target interaction.

Although it is difficult to determine if broad-spectrum DNA-interaction is a compound's definitive mechanism of cytotoxicity, it is clear that DNA interaction has a measurable influence on the mechanism. Small molecules that bind to DNA do not necessarily interact in the same way, in fact, there are several modes by which a ligand can bind and affect the structure and function of this substrate (23). Of these modes, intercalation is most prevalent with planar polycyclic aromatic systems like the aaptamines which insert between adjacent base-pairs of intact DNA, depending primarily on p-bond interactions and sometimes stacking several molecules together in the same area between base pairs.

The quinoline portion found in aaptamine's tri-cyclic core has already been the focus of SAR studies with derivatives of acridine (24), a structure that resembles aaptamine and is a well studied anti-cancer pharmacophore that intercalates DNA. The observed DNA binding activity of aaptamine may serve to explain some aspects of the compound's mechanism of activity against whole cell and viral pathogens.

Considering the high availability of the natural material and the remarkably broad activity displayed, this heterocyclic small molecule has excellent potential as a scaffold from which numerous derivatives can be made in an attempt to improve selectivity and pharmacokinetics.

Based on the synthetic work already published by Shen *et al*. (18), Hibino *et al*. (12), Pettit *et al*. (25,26) and Gul *et al*. (27) a preliminary SAR has been developed for the aaptamine scaffold in regard to cytotoxicity, antiviral and antimicrobial activity. Table 1 summarizes what has been learned of this relationship from the synthetic and natural derivatives of aaptamine.

Utilizing the information from this SAR, a semi-synthetic series of *N*-alkyl aaptamine derivatives was produced to complement previously published *N*-alkylation efforts that improved activity, and to investigate the effects of increasing the lipophilic character of the pharmacophore. In addition, it was proposed that selective demethylation of the C-9 hydroxyl would significantly increase the potency of the first generation *N*-alkyl derivatives. Our speculation was based on the evidence wherein **2** consistently demonstrated higher potency than **1** in a variety of biological assays; likewise the selective demethylation of the aaptamine derivatives would produce isoaaptamine analogs with higher potency. Two smaller groups of analogs were specifically produced to investigate the effect of dimerization on biological activity and the pro-drug behavior of sulfonyl esters relative to those previously studied.

Methods and Materials

Sponge collection and taxonomy

The sponge was collected from reef slopes at about 20 m depth, from Derawan Island and Manado Bay, Indonesia. In life the sponge forms a dense, tough, tuber-like mass, with a relatively smooth surface that may be pitted and feels like sandpaper to the touch. In life the sponge is dark orange, the interior deep yellow, the sponge oxidizes to a deep dark gold color, rendering the preservative fluorescent dark gold. The skeleton consists of large strongyloxeas in three size categories, disposed radially in the ectosome and throughout the choanosome. The sponge is *Aaptos nigra* Lévi, 1961 (Demospongiae: Hadromerida: Suberitidae), first described from Vietnam. A voucher specimen has been deposited in the Natural History Museum, London (BMNH 2005.2.16.1).

Isolation of aaptamines

The sponge *Aaptos nigra* (30 kg, wet) was extracted with 95% EtOH. Aaptamine (200 g, 1.9%) and isoaaptamine (230 g, yield 2.2%) were purified from the crude extract by VLC and MPLC using normal phase conditions analogous to several previously published procedures. As needed, additional purification was performed using reverse phase HPLC, affording smaller amounts of **1** and **2** of high purity.

Synthesis

General—With the exception of the demethylation chemistry, all reactions were performed under a nitrogen atmosphere. Reaction media were either utilized from anhydrous solvent containers obtained from Sigma-Aldrich Co. or dried through typical laboratory protocols. All reagents were purchased from Sigma-Aldrich as well. Parallel synthesis was achieved with the Firstmate® 12 unit parallel synthesizer (Argonaut Technologies, Inc.). Unless stated otherwise, reaction and purification monitoring was done using thin layer chromatography with silica gel 60 F254 aluminum-backed sheets (Merck KGaA) and visualized with long wave UV (365 nm). Flash column chromatography was performed with silica gel 60 (particle size 40–63 mm, 230–400 mesh, Silicycle Inc.). Preparative gel chromatography was performed using Sephadex LH-20 (GE Healthcare Bio-Sciences Corp.). All ^{1}H and ^{13}C NMR spectra were acquired on the Bruker DRX 400 MHz Spectrometer using XWinNMR software and an internal solvent calibration. High resolution mass spectra were acquired on the Bruker ESI-micrOTOF in positive mode coupled with an Agilent HPLC. All synthetic procedures are summarized in Scheme 1.

Parallel N-Alkylation—In each reaction tube of the parallel synthesizer, 200 mg (0.88 mmol) of **1** was dissolved in DMF (20 mL) at 0 °C. To the solution, approximately 3 equivalents of KH were added and the mixture was stirred for 10 min after which 1.2 equivalents of the appropriate alkyl iodide was added drop-wise. The reaction was stirred for an additional hour and then allowed to warm to room temperature. While at room temperature, the reaction was monitored by TLC to insure complete conversion of the starting material which occurred usually after 18–24 h. Workup consisted of aqueous extraction with $CHCl_3$, a brine wash and drying over Na_2SO_4 before evaporation under reduced pressure. Final purification was completed on a silica flash column using 5% MeOH

in ammonia saturated DCM which in most cases provided two regioisomers that required multiple repetitions of the same chromatography step to purify. Scale up of some selected derivatives was required for further study.

Sulfonylation—In a round bottom flask, 200 mg (0.88 mmol) of **2** was suspended in DCM (15 mL). To the solution, approximately two equivalents of Et_3N was added and allowed to stir for ten minutes at room temperature. The mixture was cooled to 0 °C and a DCM solution (5 mL) containing 1.2 equivalents of the appropriate sulfonyl chloride were added drop-wise over ten minutes. The reaction was stirred for an additional hour and then allowed to warm to room temperature. The solvent was removed under reduced pressure and purification was completed on a flash column with 10% MeOH in DCM.

Dimerization—In a round bottom flask fitted with a condenser, 200 mg (0.88 mmol) of **2** and cesium carbonate was suspended in acetone (40 mL). To the solution, 0.5 equivalents of the appropriate dibromoalkane were added and the mixture was refluxed while stirring to thoroughly maintain the suspension. The product precipitated from acetone and the reaction was complete when the starting compound was not detected in the solvent using mass spectrometry. Purification consisted of filtering the product from acetone, reconstituting the product in MeOH and purification by LH20 in MeOH.

Demethylation—Two methods were used for the synthesis of the demethylated aaptamines. Method A utilized BBr_3 to produce 8,9-demethylaaptamine (**30**). Method B is previously described (26), and utilized hydrobromic acid with controlled heating to selectively demethylate the 9-*O* methyl function of aaptamine.

For method A, 200 mg (0.88 mmol) of **1** was suspended in DCM (25 mL) in a round bottom flask at 0 °C. To the suspension, four equivalents of BBr_3 (1.0M in DCM) was added over 10 min. The mixture was allowed to warm to room temperature and stirred for 3 h. The solid material was filtered from the reaction and washed with DCM to give a green precipitate which was purified by LH20 in MeOH.

For method B, 200 mg of 1*N*,4*N*-didodecylaaptamine (**21**) (0.35 mmol) was added to a round bottom flask. The material was suspended with 3–4 mL 48% HBr and heated at 115 °C for approximately 30 min with stirring. The reaction was quenched with 1–2 mL water and extracted with $CHCl_3$. The organic layer was washed with brine solution and dried over Na_2SO_4. Usual column chromatography (10% MeOH in DCM) afforded 165.6 mg of compound **30**.

8,9-Dimethoxy-1-methyl-1H-benzo[de][1,6]naphthyridine (1*N*-methylaaptamine) (5): Yellow amorphous solid. Yield 21%. ^{1}H NMR (CD_3OD) δ 3.55 (s, 3H, NCH_3), 3.69 (s, 3H, OCH_3 - 9), 3.74 (s, 3H, OCH_3 - 8), 6.32 (d, J = 7.6, 1H, H - 3), 6.48(s, 1H, H - 7), 6.49(d, J = 6.4, 1H, H - 6), 7.00 (d, J = 7.6, 1H, H - 2), 7.18 (d, J = 6.8, 1H, H - 5); ^{13}C NMR (CD_3OD) δ 44.8, 55.9, 62.0, 99.7, 101.7, 112.9, 118.5, 132.9, 133.6, 134.3, 134.4, 145,3, 150.2, 158.0; HR-ESI-MS *m/z* 243.1167 (obsd), 243.1134 (calcd for $C_{14}H_{15}O_2N_2$).

8,9-Dimethoxy-4-methyl-4H-benzo[de][1,6]naphthyridine (4*N*-methylaaptamine) (6): Yellow amorphous solid. Yield 34%. HR-ESI-MS *m/z*, H^1 and C^{13}-NMR δ values match those previously reported (26).

1-Ethyl-8,9-dimethoxy-1H-benzo[de][1,6]naphthyridine (1*N*-ethylaaptamine) (7): Yellow amorphous solid. Yield 29%. ^{1}H NMR (CD_3OD) δ 1.28 (t, *J* = 6.8, 3H, NCH_3 - 2′), 3.73 (s, 3H, OCH_3 - 9), 3.91 (s, 3H, OCH_3 - 8), 4.13 (q, *J* = 7.2, 2H, NCH_2 - 1′), 6.32 (d, *J* = 7.6, 1H, H - 3), 6.65(s, 1H, H - 7), 6.71(d, *J* = 6, 1H, H - 6), 7.06 (d, *J* = 7.6, 1H, H - 2), 7.46 (d, *J* = 6.4, 1H, H - 5); ^{13}C NMR (CD_3OD) δ 15.7, 52.1, 56.6, 62.1, 99.5, 105.9, 114.7, 121.5, 133.5, 134.8, 137.1, 140.8, 144.4, 154.3, 159.0; HR-ESI-MS *m/z* 257.1320 (obsd), 257.1290 (calcd for $C_{15}H_{17}O_2N_2$).

4-Ethyl-8,9-dimethoxy-4H-benzo[de][1,6]naphthyridine (4*N*-ethylaaptamine) (8): Yellow amorphous solid. Yield 41%. ^{1}H NMR ($CDCl_3$) δ 1.22 (t, *J* = 7.2, 3H, NCH_3 - 2″) 3.67 (q, *J* = 6.4, 2H, NCH_2 - 1″), 3.78 (s, 3H, OCH_3 - 9), 3.87 (s, 3H, OCH_3 - 8), 6.05 (d, *J* = 6.4, 1H, H - 3), 6.23(d, *J* = 7.6, 1H, H - 6), 6.55(s, 1H, H - 7), 6.73(d, *J* = 7.6, 1H, H - 5), 7.91 (d, *J* = 6, 1H, H - 2); ^{13}C NMR ($CDCl_3$) δ 12.9, 48.0, 56.8, 60.9, 96.5, 101.3, 112.0, 119.6, 132.1, 134.0, 136.8, 142.5, 149.1, 149.9, 156.1; HR-ESI-MS *m/z* 257.1327 (obsd), 257.1290 (calcd for $C_{15}H_{17}O_2N_2$).

8,9-Dimethoxy-1-propyl-1H-benzo[de][1,6]naphthyridine (1*N*-propylaaptamine) (9): Yellow amorphous solid. Yield 30%. ^{1}H NMR ($CDCl_3$) δ 0.88 (t, *J* = 7.6, 3H, NCH_3 - 3′), 1.66 (dt, *J* = 7.2, 2H, NCH_2 - 2′), 3.69 (s, 3H, OCH_3 - 9), 3.90 (s, 3H, OCH_3 - 8), 3.98 (t, *J* = 7.6, 2H, NCH_2 - 1′), 5.94 (d, *J* = 7.6, 1H, H - 3), 6.60 (s, 1H, H - 7), 6.71 (d, *J* = 6, 1H, H - 6), 6.96 (d, *J* = 7.6, 1H, H - 2), 7.53 (d, *J* = 6.4, 1H, H - 5); ^{13}C NMR ($CDCl_3$) δ 11.2, 24.0, 56.5, 58.4, 62.1, 98.9, 106.3, 114.7, 121.8, 133.2, 134.8, 137.3, 142.6, 144.2, 154.9, 158.7; HR-ESI-MS *m/z* 271.1484 (obsd), 271.1447 (calcd for $C_{16}H_{19}O_2N_2$).

8,9-Dimethoxy-4-propyl-4H-benzo[de][1,6]naphthyridine (4*N*-propylaaptamine) (10): Yellow amorphous solid. Yield 32%. ^{1}H NMR ($CDCl_3$) δ 0.95 (t, *J* = 7.2, 3H, NCH_3 - 3″), 1.66 (dt, *J* = 7.6, 2H, NCH_2 - 2″) 3.57 (t, *J* = 7.2, 2H, NCH_2 - 1″), 3.79 (s, 3H, OCH_3 - 9), 3.88 (s, 3H, OCH_3 - 8), 6.04 (d, *J* = 6, 1H, H - 3), 6.19 (d, *J* = 7.2, 1H, H - 6), 6.58 (s, 1H, H - 7), 6.69 (d, *J* = 7.2, 1H, H - 5), 8.00 (d, *J* = 5.6, 1H, H - 2); ^{13}C NMR ($CDCl_3$) δ 11.2, 21.3, 54.3, 56.7, 60.8, 96.5, 101.1, 120.1, 132.2, 134.8, 137.8, 144.7, 149.2, 151.6, 155.8; HR-ESI-MS *m/z* 271.1483 (obsd), 271.1447 (calcd for $C_{16}H_{19}O_2N_2$).

1-Butyl-8,9-dimethoxy-1H-benzo[de][1,6]naphthyridine (1N-butylaaptamine) (11): Yellow amorphous solid. Yield 24%. ^{1}H NMR ($CDCl_3$) δ 0.88 (t, *J* = 7.6, 3H, NCH_3 - 4′), 1.31 (s, *J* = 7.6, 2H, NCH_2 - 3′), 1.66 (p, *J* = 7.6, 2H, NCH_2 – 2′), 3.71 (s, 3H, OCH_3 - 9), 3.92 (s, 3H, OCH_3 - 8), 4.01 (t, *J* = 7.6, 2H, NCH_2 - 1′), 6.21 (d, *J* = 7.6, 1H, H - 3), 6.49 (s, 1H, H - 7), 6.69 (d, *J* = 6, 1H, H - 6), 6.78 (d, *J* = 7.6, 1H, H - 2), 7.71 (d, *J* = 6, 1H, H - 5); ^{13}C NMR ($CDCl_3$) δ 13.8, 19.8, 31.7, 56.0, 61.6, 97.5, 106.4, 113.3, 120.6, 131.7, 133.8, 135.8, 141.6, 142.3, 153.1, 157.0; HR-ESI-MS *m/z* 285.1642 (obsd), 285.1603 (calcd for $C_{17}H_{21}O_2N_2$).

4-Butyl-8,9-dimethoxy-4H-benzo[de][1,6]naphthyridine (4N-butylaaptamine) (12): Yellow amorphous solid. Yield 40%. ^{1}H NMR ($CDCl_3$) δ 0.89 (t, J = 7.6, 3H, NCH_3 - 4″), 1.66 (s, J = 7.6, 2H, NCH_2 - 3″), 1.62 (p, J = 7.6, 2H, NCH_2 - 2″), 3.64 (t, J = 7.6, 2H, NCH_2 - 1″), 3.87 (s, 3H, OCH_3 - 9), 3.88 (s, 3H, OCH_3 - 8), 5.96 (d, J = 6, 1H, H - 3), 6.28 (d, J = 7.6, 1H, H - 6), 6.53 (s, 1H, H - 7), 6.67 (d, J = 7.6, 1H, H - 5), 8.18 (d, J = 5.6, 1H, H - 2); ^{13}C NMR ($CDCl_3$) δ 13.7, 19.7, 29.0, 52.2, 56.3, 60.7, 95.2, 100.8, 110.8, 118.4, 130.5, 133.4, 135.8, 140.7, 148.0, 148.5, 154.9; HR-ESI-MS *m/z* 285.1641 (obsd), 285.1603 (calcd for $C_{17}H_{21}O_2N_2$).

8,9-Dimethoxy-1-(3-methyl-butyl)-1H-benzo[de][1,6]naphthyridine [1*N*-(3-methylbutyl)aaptamine] (13): Yellow amorphous solid. Yield 26%. ^{1}H NMR ($CDCl_3$) δ 0.92 (d, J = 6, 6H, (1) NCH_3 - 4′), 1.61 (m, 1H, NCH - 3′), 1.61 (m, 2H, NCH_2 – 2′), 3.77 (s, 3H, OCH_3 - 9), 3.98 (s, 3H, OCH_3 - 8), 4.18 (t, J = 7.6, 2H, NCH_2 - 1′), 6.67 (s, 1H, H - 7), 6.68 (m, 1H, H - 3), 6.69 (d, J = 6.8, 1H, H - 6), 7.14 (d, J = 8, 1H, H - 2), 7.49 (d, J = 6.4, 1H, H - 5); ^{13}C NMR ($CDCl_3$) δ 22.5, 26.0, 38.8, 55.9, 56.4, 61.8, 99.8, 103.3, 113.4, 119.5, 133.0, 133.8, 134.7, 135.2, 144.7, 150.9, 158.2; HR-ESI-MS *m/z* 299.1800 (obsd), 299.1759 (calcd for $C_{18}H_{23}O_2N_2$).

8,9-Dimethoxy-4-(3-methyl-butyl)-4H-benzo[de][1,6]naphthyridine [4*N*-(3-methylbutyl)aaptamine] (14): Yellow amorphous solid. Yield 33%. ^{1}H NMR ($CDCl_3$) δ 0.95(d, J = 6.4, 6H, NCH_3 - 4″,5″), 1.53 (q, J = 7.6, 2H, NCH_2 - 2″), 1.65 (m, 1H, NCH_2 - 3″), 3.53 (t, J = 7.6, 2H, NCH_2 - 1″), 3.89 (s, 3H, OCH_3 - 8), 3.91 (s, 3H, OCH_3 - 9), 5.89 (d, J = 6 Hz, 1H, H - 6), 6.09 (d, J = 7.6 Hz, 1H, H - 5), 6.45 (s, 1H, H - 7), 6.46 (d, J = 7.6 Hz, 1H, H - 3), 8.26 (d, J = 6 Hz, 1H, H - 2); ^{13}C NMR ($CDCl_3$) δ 22.5, 25.9, 35.5, 50.3, 56.3, 60.5, 95.1, 99.9, 109.4, 119.1, 130.1, 132.9, 137.6, 144.5, 147.3, 151.5, 154.0; HR-ESI-MS *m/z* 299.1802 (obsd), 299.1759 (calcd for $C_{18}H_{23}O_2N_2$).

4-Hexyl-8,9-dimethoxy-4H-benzo[de][1,6]naphthyridine (4N-hexylaaptamine) (15): Yellow amorphous solid. Yield 68%. ^{1}H NMR ($CDCl_3$) δ 0.84 (t, J = 6.8, 3H, NCH_3 - 7″), 1.28 (m, 8H, NCH_2 - 4″ - 5″), 1.38 (m, 2H, NCH_2 – 3″) 1.74 (bt, 2H, NCH_2 - 2″), 3.97 (s, 3H, OCH_3 - 8), 4.00 (m, 2H, NCH_2 - 1″), 4.00 (s, 3H, OCH_3 - 9), 6.30 (d, J = 7.2 Hz, 1H, H - 3), 6.82 (d, J = 7.6 Hz, 1H, H - 6), 6.90 (s, 1H, H - 7), 7.12 (d, J = 7.2 Hz, 1H, H - 5),8.22 (d, J = 7.2 Hz, 1H, H - 2); ^{13}C NMR ($CDCl_3$) δ 153.8, 151.6, 147.2, 144.8, 137.5, 133.1, 130.1, 119.0, 109.0, 99.6, 95.0, 60.4, 56.2, 51.9, 31.7, 29.0, 26.7, 26.6, 22.6, 14.1; HR-ESI-MS *m/z* 313.1951 (obsd), 313.1916 (calcd for $C_{19}H_{25}O_2N_2$).

1-Heptyl-8,9-dimethoxy-1H-benzo[de][1,6]naphthyridine (1N-heptylaaptamine) (16): Yellow amorphous solid. Yield 40%. ^{1}H NMR ($CDCl_3$) δ 0.92 (t, J = 6.8, 3H, NCH_3 - 7′), 1.34 (m, 8H, NCH_2 - 3′ - 6′), 1.73 (bt, 2H, NCH_2 - 2′), 3.78 (s, 3H, OCH_3 - 9), 3.99 (s, 3H, OCH_3 - 8), 4.14 (t, J = 7.6, 2H, NCH_2 - 1′), 6.05 (d, J = 7.6, 1H, H - 3), 6.75 (s, 1H, H - 7), 6.81 (d, J = 6, 1H, H - 6), 7.12 (d, J = 7.6, 1H, H - 2), 7.57 (d, J = 6.4, 1H, H - 5); ^{13}C NMR ($CDCl_3$) 14.5, 23.7, 27.5, 30.2, 30.8, 33.0, 56.6, 57.1, 62.1, 99.4, 105.8, 114.7, 121.6, 133.5, 134.9, 137.2, 141.4, 144.8, 154.5, 159.0; HR-ESI-MS *m/z* 327.2097 (obsd), 327.2072 (calcd for $C_{20}H_{27}O_2N_2$).

4-Heptyl-8,9-dimethoxy-4H-benzo[de][1,6]naphthyridine (4N-heptylaaptamine) (17): Yellow amorphous solid. Yield 36%. ^{1}H NMR ($CDCl_3$) δ 0.83 (t, J = 6.8, 3H, NCH_3 - 7″), 1.25 (m, 8H, NCH_2 - 3″ - 6″), 1.62 (bt, 2H, NCH_2 - 2″), 3.47 (t, J = 7.2, 2H, NCH_2 - 1″), 3.88 (s, 3H, OCH_3 - 8), 3.91 (s, 3H, OCH_3 - 9), 5.87 (d, J = 5.6 Hz, 1H, H - 6), 6.01 (d, J = 7.6 Hz, 1H, H - 5), 6.39 (d, J = 8 Hz, 1H, H - 3), 6.41 (s, 1H, H - 7), 8.25 (d, J = 5.6 Hz, 1H, H - 2); ^{13}C NMR ($CDCl_3$) δ 153.8, 151.6, 147.2, 144.8, 137.5, 133.1, 130.1, 119.0, 109.0, 99.6, 95.0, 60.4, 56.2, 51.9, 31.7, 29.0, 26.7, 26.6, 22.6, 14.1; HR-ESI-MS *m/z* 327.2105 (obsd), 327.2072 (calcd for $C_{20}H_{27}O_2N_2$).

8,9-Dimethoxy-1-nonyl-4H-benzo[de][1,6]naphthyridine (1*N*-nonylaaptamine) (18): Yellow amorphous solid. Yield 35%. ^{1}H NMR ($CDCl_3$) δ 0.85 (t, J = 6.8, 3H, NCH_3 - 9′), 1.24 (m, 12H, NCH_2 - 3′ - 8′), 1.67 (bs, 2H, NCH_2 - 2′), 3.71 (s, 3H, OCH_3 - 9), 3.92 (s, 3H, OCH_3 - 8), 3.96 (t, J = 7.6, 2H, NCH_2 - 1′), 6.08 (d, J = 8, 1H, H - 3), 6.45 (s, 1H, H - 7), 6.68 (d, J = 7.2, 1H, H - 2), 6.70 (d, J = 6, 1H, H - 6), 7.78 (d, J = 5.6, 1H, H - 5); ^{13}C NMR ($CDCl_3$) 14.2, 22.7, 26.6, 29.3, 29.4, 29.6, 29.7, 31.9, 55.9, 56.0, 61.5, 96.6, 107.5, 109.9, 113.3, 121.0, 131.5, 133.8, 135.9, 141.6, 143.7, 153.8, 156.8; HR-ESI-MS *m/z* 355.2423 (obsd), 355.2385 (calcd for $C_{22}H_{31}O_2N_2$).

8,9-Dimethoxy-4-nonyl-4H-benzo[de][1,6]naphthyridine (4*N*-nonylaaptamine) (19): Yellow amorphous solid. Yield 45%. ^{1}H NMR ($CDCl_3$) δ 0.85 (t, J = 7.2, 3H, NCH_3 - 9″), 1.27 (m, 12H, NCH_2 - 3″ - 8″), 1.66 (bs, 2H, NCH_2 - 2″), 3.51 (t, J = 7.6, 2H, NCH_2 - 1″), 3.90 (s, 3H, OCH_3 - 8), 3.91 (s, 3H, OCH_3 - 9), 5.89 (d, J = 6 Hz, 1H, H - 6), 6.06 (d, J = 7.2 Hz, 1H, H - 5), 6.43 (d, J = 7.6 Hz, 1H, H - 3), 6.43 (s, 1H, H - 7), 8.24 (d, J = 5.6 Hz, 1H, H - 2); ^{13}C NMR ($CDCl_3$) δ 14.2, 22.7, 26.7, 29.3, 29.3, 29.5, 31.9, 50.7, 51.9, 56.3, 60.5, 95.2, 99.8, 109.0, 119.1, 130.1, 133.1, 137.9, 145.1, 147.2, 151.9, 153.8; HR-ESI-MS *m/z* 355.2419 (obsd), 355.2385 (calcd for $C_{22}H_{31}O_2N_2$).

1-Dodecyl-8,9-dimethoxy-4H-benzo[de][1,6]naphthyridine (1*N*-dodecylaaptamine) (20): Yellow amorphous solid. Yield 24%. ^{1}H NMR ($CDCl_3$) δ 0.85 (t, J = 6.8, 3H, NCH_3 - 12′), 1.20 (bs, 18H, NCH_2 - 3′ - 11′), 1.65 (bs, 2H, NCH_2 - 2′), 3.69 (s, 3H, OCH_3 - 9), 3.90 (s, 3H, OCH_3 - 8), 3.93 (t, J = 6.4, 2H, NCH_2 - 1′), 6.05 (d, J = 7.6, 1H, H - 3), 6.43 (s, 1H, H - 7), 6.66 (d, J = 7.6, 1H, H - 2), 6.68 (d, J = 6, 1H, H - 6), 7.77 (d, J = 5.6, 1H, H - 5); ^{13}C NMR ($CDCl_3$) 14.2, 22.8, 26.6, 29.6 (6), 32.0, 55.9, 61.5, 96.8, 107.5, 113.3, 121.0, 131.4, 133.8, 135.9, 141.6, 143.8, 153.8, 156.7; HR-ESI-MS *m/z* 397.2882 (obsd), 397.2855 (calcd for $C_{25}H_{37}O_2N_2$).

1,4-Didodecyl-8,9-dimethoxy-4H-benzo[de][1,6]naphthyridin-1-ium Iodide (1*N*,4*N*-didodecylaaptamine as iodide salt) (21): Yellow amorphous solid. Yield 69% ^{1}H NMR ($CDCl_3$) δ 0.75 (t, J = 6.8, 6H, NCH_3 – 12′, 12″), 1.28 (m, 36H, NCH_2-3′ – 11′, 3″ – 11″), 1.68 (m, 4H, NCH_2 – 2′, 2″), 4.02 (t, J = 7.6, 2H, NCH_2 – 1″), 4.40 (t, J = 7.6, 2H, NCH_2 – 1′), 3.75 (s, 3H, OCH_3 - 9), 3.98 (s, 3H, OCH_3 - 8), 6.55 (d, J = 8 Hz, 1H, H - 3), 6.98 (d, J = 7.2 Hz, 1H, H - 6), 7.09 (s, 1H, H - 7), 7.31 (d, J = 7.2 Hz, 1H, H - 5), 8.23 (d, J = 5.6 Hz, 1H, H - 2); ^{13}C NMR ($CDCl_3$) δ 14.0, 22.5, 26.2, 26.3, 27.7, 29.4, 30.3, 31.8, 54.3, 57.0, 58.4, 62.1, 97.7, 102.8, 114.8, 119.1, 133.0, 133.1, 134.1, 134.3, 148.6, 149.4, 158.5; HR-ESI-MS *m/z* 565.4754 (obsd), 565.4733 (calcd for $C_{37}H_{61}O_2N_2$).

4-Hexadecyl-8,9-dimethoxy-4H-benzo[de][1,6]naphthyridine (4*N*-hexadecylaaptamine) (22): Yellow amorphous solid. Yield 60%. ^{1}H NMR ($CDCl_3$) δ 0.87 (t, J = 7.2, 3H, NCH_3 - 12″), 1.29 (m, 18H, NCH_2 -3″ - 15″), 1.69 (bs, 2H, NCH_2 - 2″), 3.58 (t, J = 7.2, 2H, NCH_2 - 1″), 3.93 (s, 3H, OCH_3 - 8), 3.96 (s, 3H, OCH_3 - 9), 5.95 (d, J = 6 Hz, 1H, H - 3), 6.15 (d, J = 7.6 Hz, 1H, H - 6), 6.50 (s, 1H, H - 7), 6.51 (d, J = 7.6 Hz, 1H, H - 5), 8.29 (d, J = 6 Hz, 1H, H - 2); ^{13}C NMR ($CDCl_3$) δ 14.3, 22.8, 26.8, 26.9, 29.4, 29.5, 29.6, 29.7, 29.7, 29.8, 32.1, 52.2, 56.4, 60.7, 95.2, 100.1, 109.6, 119.1, 130.2, 133.1, 137.6, 147.6, 151.1, 154.3; HR-ESI-MS *m/z* 453.3508 (obsd), 453.3481 (calcd for $C_{29}H_{45}O_2N_2$).

8-methoxy-1-methyl-1H-benzo[de][1,6]naphthyridin-9-yl methyl-1-sulfonate (9-*O*-methylsulfonylisoaaptamine) (23): Yellow amorphous solid. Yield 67%. ^{1}H NMR (CD_3OD) δ 3.34 (s, 3H, CH_3 – 1′), 3.72 (s, 3H, NCH_3), 3.94 (s, 3H, OCH_3 - 8), 6.08 (d, J = 6.8 Hz, 1H, H - 5), 6.64 (s, 1H, H - 7), 6.84 (bd, 1H, H - 6), 7.03(d, J = 6.8 Hz, 1H, H - 2), 7.69 (bd, 1H, H - 3); ^{13}C NMR (CD_3OD) δ 39.9, 45.1, 56.7, 98.1, 107.7, 114.7, 121.0, 122.4, 138.3, 139.3, 143.9, 144.6, 154.4, 157.7; HR-ESI-MS *m/z* 307.0801 (obsd), 307.0747 (calcd for $C_{14}H_{15}O_4N_2S$).

8-Methoxy-1-methyl-1H-benzo[de][1,6]naphthyridin-9-yl propane-1-sulfonate (9-*O*-propylsulfonylisoaaptamine) (24): Yellow amorphous solid. Yield 80%. ^{1}H NMR (CD_3OD) δ 1.09 (t, J = 8 Hz, 3H, CH_3 – 3′), 2.01 (m, 2H, CH_2 – 2′), 3.37 (t, J = 8 Hz, 2H, CH_2 – 1′), 3.70 (s, 3H, NCH_3), 3.88 (s, 3H, OCH_3 - 8), 6.25 (d, J = 7.2 Hz, 1H, H - 5), 6.45 (s, 1H, H - 7), 6.72 (d, J = 6.4 Hz, 1H, H - 6), 6.81 (d, J = 7.6 Hz, 1H, H - 2), 7.77 (d, J = 6 Hz, 1H, H - 3); ^{13}C NMR (CD_3OD) δ 13.0, 17.5, 44.8, 54.4, 56.1, 97.0, 107.1, 113.3, 119.7, 120.7, 137.1, 142.4, 142.7, 152.3, 155.9; HR-ESI-MS *m/z* 335.1103 (obsd), 335.1060 (calcd for $C_{16}H_{19}O_4N_2S$).

8-Methoxy-1-methyl-1H-benzo[de][1,6]naphthyridin-9-yl octane-1-sulfonate (9-*O*-octylsulfonylisoaaptamine) (25): Yellow amorphous solid. Yield 46%. ^{1}H NMR ($CDCl_3$) δ 0.87 (t, J = 6.4, 3H, CH_3 – 7′), 1.30 (m, 9H, CH_3 – 8′ and CH_2 – 4′, 5′, 6′), 1.49 (m, 2H, CH_2 – 3′), 2.02 (m, 2H, CH_2 – 2′), 3.45 (t, J = 6.8 Hz, 2H, CH_2 – 1′), 3.89 (s, 3H, NCH_3), 3.98 (s, 3H, OCH_3 - 8), 6.70 (m, 2H, H – 7, 5), 6.81 (d, J = 6.4 Hz, 1H, H - 6), 7.18 (d, J = 7.6 Hz, 1H, H - 2), 7.58 (d, J = 6 Hz, 1H, H - 3); ^{13}C NMR ($CDCl_3$) δ 14.2, 22.7, 23.7, 28.4, 29.0, 29.1, 29.3, 29.4, 31.8, 45.8, 53.2, 56.6, 99.3, 104.2, 113.5, 118.9, 121.8, 136.8, 137.5, 145.0, 150.4, 157.3; HR-ESI-MS *m/z* 405.1893 (obsd), 405.1848 (calcd for $C_{21}H_{29}O_4N_2S$).

8-Methoxy-1-methyl-1H-benzo[de][1,6]naphthyridin-9-yl phenylmethane-sulfonate (9-*O*-phenylsulfonylisoaaptamine) (26): Yellow amorphous solid. Yield 62%. ^{1}H NMR (CD_3OD) δ 3.32 (s, 3H, NCH_3), 3.45 (s, 2H, OCH_2), 3.80 (s, 3H, OCH_3 - 8), 6.36 (s, 1H, H - 7), 6.50 (d, J = 7.2 Hz, 1H, H - 5), 6.74 (d, J = 6.4 Hz, 1H, H - 6), 6.98 (d, J = 7.2 Hz, 1H, H - 2), 7.55 (t, J = 8 Hz, 2H, m-Ph-S) 7.67 (t, J = 7.2, 1H, p-Ph-S), 7.75 (d, J = 6.4, 1H, H – 3) 7.69 (d, J = 7.6, 2H, *o*-Ph-S); ^{13}C NMR (CD_3OD) δ 45.2, 50.7, 55.5, 97.5, 106.2, 113.4, 119.3, 121.3, 126.1, 128.3, 128.6, 129.0, 134.3, 136.8, 137.2, 137.6, 140.5, 143.3, 151.6, 156.5; HR-ESI-MS *m/z* 383.1051(obsd), 383.1060 (calcd for $C_{20}H_{19}O_4N_2S$).

1,6-Bis-(8-methoxy-1-methyl-1H-benzo[de][1,6]naphthyridin-9-yloxy)-hexane (1,6-bisisoaaptamine hexane) (27): Yellow amorphous solid. Yield 89%. ^{1}H NMR (CD_3OD)

(*resonance overlap) δ 1.52 (bs, 4H, CH_2 - 3′, 3″), 1.75 (bs, 4H, CH_2 – 2′, 2″), 3.67 (s, 6H, NCH_3*), 3.79 (t, J = 6.4 Hz, 4H, OCH_2 – 1′, 1″), 3.86 (s, 6H, OCH_3 – 8*), 5.86 (s, J = 8 Hz, 2H, H – 5*), 6.52 (s, 2H, H – 7*), 6.67 (d, J = 6.4 Hz, 2H, H – 6*), 6.84 (d, J = 8 Hz, 1H, H – 2*), 7.51 (d, J = 6.4 Hz, 2H, H – 3*); ^{13}C NMR (CD_3OD) δ 27.0*, 30.9*, 44.6*, 56.4*, 75.9*, 98.5*, 106.4*, 114.6*, 121.6*, 132.2*, 136.4*, 137.1*, 143.3*, 144.2*, 155.0*, 158.7*; HR-ESI-MS *m/z* 540.2706 (obsd), 540.2736 (calcd for $C_{32}H_{36}O_4N_4$).

1,9-Bis-(8-methoxy-1-methyl-1H-benzo[de][1,6]naphthyridin-9-yloxy)-nonane (1,9-Bisisoaaptamine nonane) (28): Yellow amorphous solid. Yield 96%. ^{1}H NMR (CD_3OD) (*resonance overlap) δ 1.38 (bs, 6H, CH_2 - 4′, 4″ and CH_2 - 5′), 1.47 (bs, 4H, CH_2 – 3′, 3″), 1.73 (m, 4H, CH_2 – 2′,2″), 3.69 (s, 6H, NCH_3*), 3.79 (t, J = 6.4 Hz, 4H, OCH_2 – 1′, 1″), 3.87 (s, 6H, OCH_3 – 8*), 5.87 (s, J = 8 Hz, 2H, H – 5*), 6.54 (s, 2H, H – 7*), 6.68 (d, J = 6.4 Hz, 2H, H – 6*), 6.85 (d, J = 8 Hz, 1H, H – 2*), 7.52 (d, J = 6.4 Hz, 2H, H – 3*); ^{13}C NMR (CD_3OD) δ 27.1*, 30.4*, 30.6, 30.8*, 44.6*, 56.4*, 76.0*, 98.5*, 106.4*, 114.6*, 121.6*, 132.3*, 136.4*, 137.1*, 143.1*, 144.2*, 155.0*, 158.7*; HR-ESI-MS *m/z* 581.3107 (obsd), 581.3127 (calcd for $C_{35}H_{41}O_4N_4$).

1H-Benzo[de][1,6]naphthyridine-8,9-diol (8,9-demethylaaptamine) (29): Green amorphous powder. Yield 99%. HR-ESI-MS *m/z*, H^1 and C^{13}-NMR δ match those previously reported (26).

1,4-Didodecyl-8-methoxy-9-hydroxy-1H-benzo[de][1,6]naphthyridin-4-ium bromide (9-*O*-demethyl-1*N*,4*N*-didodecylaaptamine, as bromide salt) (30): Yellow amorphous solid. Yield 82%. ^{1}H NMR ($CDCl_3$) δ 0.69 (t, J = 6.8, 3H, NCH_3 – 12), 1.06 (m, 36H, NCH_2 – 3–10, 3–11), 1.25 (t, J = 7.6, 3H, NCH_3 - 12) 1.60 (m, 4H, NCH_2 – 2, 2), 3.01 (q, J = 7.6, 2H, NCH_2 – 11), 3.84 (m, 2H, NCH_2 – 1), 3.92 (s, 3H, OCH_3 - 8), 4.45 (m, 2H, NCH_2 – 1), 6.13 (d, J = 6.8 Hz, 1H, H - 3), 6.65 (d, J = 7.2 Hz, 1H, H - 6), 6.82 (s, 1H, H - 7), 7.02 (d, J = 6.8 Hz, 1H, H - 5), 7.83 (d, J = 7.2 Hz, 1H, H - 2); ^{13}C NMR ($CDCl_3$) δ 8.6, 13.9, 22.4, 26.1, 26.2, 27.5, 29.1, 29.2, 29.3, 29.3, 29.4, 29.4, 31.1, 31.6, 45.9, 53.7, 56.8, 58.4, 96.0, 101.4, 114.5, 119.4, 127.4, 128.6, 132.3, 132.4, 148.8, 148.9, 152.8; HR-ESI-MS *m/z* 551.4581 (obsd), 551.4571 (calcd for $C_{36}H_{59}O_2N_2$).

DNA Binding Assay—The interaction of aaptamine with calf thymus DNA was examined by UV-vis spectrophotometry following a previously published procedure, standardized with the acridine derivative AAS (24).

Disk Diffusion Soft-Agar Colony Formation Assay for Cytotoxicity—The method used in the determination of cytotoxicity was a slight variant of a previously published procedure (28). A disk diffusion assay was used to determine the compounds selectivity for cancer cell growth inhibition. Two murine neoplasms, leukemia (L1210) and colon (Colon38), three human neoplasms, colon (H116), lung (H125) and leukemia (CCRF-CEM) along with one normal cell type (hematopoietic progenitor) were utilized. This assay focuses on a compounds ability to preferentially inhibit solid tumor cells in order to identify agents with mechanisms of action different from standard anticancer leads identified through typical in vitro screening protocols. One novelty of the assay lies in the fact that diffusion characteristics do not directly influence the observations of each individual compound's

selectivity among the neoplasms. Positive results can take several forms as selectivity can be defined between either the murine or human solid tumor cells compared to either the normal or leukemia cells. Compounds are dissolved in DMSO and 15 μL are applied to a 6.5 mm Baxter filter disk. The disk is dried overnight and a then placed near the edge of the Petri dish containing the culture and incubated for 7–10 days. Values are measured in zone units from the edge of the test disk in which 200 zone units is arbitrarily taken as 6.5 mm (the diameter of the disk). Approximately 1 mg of each compound was diluted in 0.25 mL DMSO. Solutions are diluted further (e.g. 1/4 and 1/16) if the initial test yields a zone of 750 units or more.

Results and Discussion

In all, twenty seven derivatives were synthesized for biological evaluation; Figure 2 shows the four groups of derivatives produced through semi-synthesis along with their calculated Log D values[c] demonstrating the range of increasing lipophilic or hydrophilic character in comparison Log D values for compounds **1** and **2** at 1.51 and 1.57 respectively. The isoaaptamine dimers **27** and **28** represent a preliminary attempt to improve selectivity by providing two possible sites of compound interaction with the target. The fully demethylated compound **29** has been isolated (29) and synthesized (26) previously, but has not been evaluated for its anti-viral activity. Selectively demethylated derivative **30** represents the first of the proposed second generation derivatives produced from the dialkylated compound **21**.

Table 2 summarizes the activity against microbial and AIDS related opportunistic infections. Overall, the data show that several of the *N*-alkyl analogs have potency against bacteria and are moderately active as antifungal agents. Of particular interest is the significant activity of some of the analogs against the methicillin resistant strain of *Staphylococcus aureus* (MR*Sa*). None of the alkylation products having five or less carbon units in their *N*-alkyl chains were active. The predicted Log D values for the completely inactive *N*-alkyl compounds ranged from 2.21 to 3.75, and the Log D for the most active against MR*Sa* was 6.01. The activity against MR*Sa* peaks with 1*N*-dodecyl (**20**) and then the activity diminished for derivatives **21** and **22** which have higher Log D values. It is therefore reasonable that in this homologous series, the optimal chain length should produce a Log D between 3.75 and 7.09 to be effective against MR*Sa*.

Activity against the chloroquine sensitive (D6) and resistant (W2) *Plasmodium falciparum* strains was improved (Table 3), and similar to the anti-microbial activity, notable improvement occurs with derivatives having more than five carbon units in the alkyl chain. However, there is distinct improvement in the activity seen with compound **30**. Demethylation of the C-9 methoxy of compound **21** gives over a ten fold increase in activity against the resistant strain; this supports our observations from the previous SAR studies that protection of the C-9 hydroxyl will generally decrease potency.

Although this is the first report of aaptamine derivatives having activity against *Mycobacterium tuberculosis*, the in vitro results for all derivatives ranged from moderate to inactive. In several cases though, the activity paralleled that of the less virulent

Mycobacterium intracellulare (Table 2) supporting its value as a guide for the development of anti-tuberculosis analogs.

Table 4 lists the activity of the aaptamine derivatives against HIV-1 in human peripheral blood mononuclear (PBM) cells. Cytotoxicity for PBM, T-lymphoblastoid (CEM) and African green monkey kidney (Vero) cell lines were also measured to determine the therapeutic selectivity of active derivatives. Although several of the derivatives have significantly improved activity against HIV-1, cytotoxicity for the majority of the compounds was high in comparison to the control.

Table 5 shows the observed cytotoxicity for aaptamine semi-synthetic derivatives in the disk diffusion soft-agar colony formation assay. The disk diffusion assay provided a unique analysis of relative selectivity. Compounds **11** and **14–17** showed good potency and selectivity against murine colon tumor cells versus leukemia and normal cells. In addition to this assessment, *N*-alkyl derivatives **17** and **20**, isoaaptamine dimer **2** and the demethylated derivative **30** were chosen for assessment in the 60-cell cytotoxicity panel at the National Cancer Institute. Their evaluation in this in vitro panel showed good potency but low selectivity and corresponds to the data shown for the same derivatives in the disk diffusion assay.

Aaptamine was evaluated for its ability to bind to DNA by UV-vis spectroscopy. Figure 3 shows that in addition to the pronounced decrease in absorbance intensity (hypochromicity) of aaptamine upon DNA binding, a bathochromic (red) shift in the λ_{max} of aaptamine was also observed, with λ_{max} increasing from 381 nm for the free ligand species to 391 nm as the ligand becomes bound to the DNA. This 10 nm bathochromic shift in absorbance is indicative of the formation of an intercalative complex. The inset shows the absorbance at 381 nm as a function of log [DNA]; the solid line represents the nonlinear least-squares fit of the binding isotherm model (30) to the titration data and provides an estimate of the intrinsic binding constant K_{obs}. The interaction of aaptamine with calf thymus DNA was characterized by a binding affinity of 4.0 (±0.2) × 10^3 M^{-1} (base pairs) a relatively weak binding affinity, but comparable to that reported for AAS, a known cytotoxin and DNA intercalator (24).[12] This DNA binding data, the published cytotoxicity and anti-viral activity together suggest that aaptamine utilizes DNA intercalation in its mechanism of action for these particular targets. Some analogs presented herein with improved anti-tumor, anti-microbial and anti-malarial activity could also utilize this mechanism.

Conclusions and Future Directions

The limit of chemical diversity in the marine environment is still undetermined and will continue to grow with ongoing improvements in the technology associated with collection and isolation of natural products. However, it has been demonstrated that a large number of bioactive secondary metabolites become clinical candidates through semi-synthetic optimization of their original structure (31). The simplicity of aaptamine's core structure, the potential for orally bioavailable analogs and its ability to intercalate DNA provide a unique opportunity for drug discovery. Aaptamine could be an ideal candidate for an emerging technique such as fragment-based drug design, which utilizes molecules with relatively non-

specific target interactions (32). Our studies of the currently available structure activity relationship and the knowledge gained through modifications and subsequent biological assessments contribute to the development of this pharmacophore for cancer, HIV-1 and infectious disease. Further modifications are undoubtedly necessary due to the observed cytotoxicity, not to mention improved potency against the other anti-viral and whole cell targets shown. Although the cyototoxicity appears to track activity in other whole cell assays, this is a typical result for compounds that interact with DNA. However, the intercalative function of aaptamine can become a benefit rather than a liability when used in combination with additional functionality that provides better selectivity.

Supplementary Material

Refer to Web version on PubMed Central for supplementary material.

Acknowledgements

This work was supported in part by grants from the National Institutes of Health: NIAID (R01 AI36596) and NCRR (P20 RR021929). The authors would like to thank Marsha Wright for conducting the anti-microbial testing, which was supported by the NIH, NIAID, Division of AIDS, Grant No. AI 27094, and the USDA Agricultural Research Service Specific Cooperative Agreement No. 58-6408-2-0009. Anti-malaria assays were conducted by John Trott. Additional in vitro anti-HIV data were determined at the Southern Research Institute, Frederick, MD, under NIAID Contract N01-AI-25478. This investigation was conducted in a facility constructed with support from research facilities improvement program C06 RR-14503-01 from the NIH National Center for Research Resources.

References

1. Nakamura H, Kobayashi J, Ohizumi Y, Hirata Y. Isolation and structure of aaptamine, a novel heteroaromatic substance possessing α-blocking activity from the sea sponge *Aaptos aaptos*. Tetrahedron Letters. 1982; 23:5555–5558.
2. Nakamura H, Kobayashi J, Ohizumi Y, Hirata Y. Physiologically active marine natural products from Prolifera. Part 10. Aaptamines. Novel benzo[de][1,6]naphthyridines from the Okinawan marine sponge Aaptos aaptos. J Chem Soc Perkin Trans. 1987; 1:173–176.
3. Park SK, Kim SS, Park JD, Hong JS, Kim IK. A study on the chemical constituents from marine sponge *Luffariella* sp. J Korean Chem Soc. 1995; 39:559–563.
4. Shen Y-C, Chein C-C, Hsieh P-W, Duh C-Y. Bioactive constituents from marine sponge *Aaptos aaptos*. Taiwan Shuichan Xuehuikan. 1997; 24:117–125.
5. Coutinho A, Chanas B, Souza T, Frugrulhetti I, Epifanio R. Anti HSV-1 alkaloids from a feeding deterrent marine sponge of the genus *Aaptos*. Heterocylces. 2002; 57:1265–1272.
6. Pettit GR, Hoffmann H, McNulty J, Higgs KC, Murphy A, Molloy DJ, et al. Antineoplastic agents. 380. Isolation and X-ray crystal structure determination of isoaaptamine from the Republic of Singapore *Hymeniacidon* sp. and conversion to the phosphate prodrug hystatin 1. J Nat Prod. 2004; 67:506–509. [PubMed: 15043446]
7. Calcul L, Longeon A, Al-Mourabit A, Guyot M, Bourguet-Kondracki M-L. Novel alkaloids of the aaptamine class from an Indonesian marine sponge of the genus *Xestospongia*. Tetrahedron. 2003; 59:6539–6544.
8. Sugino E, Choshi T, Hibino S. Progress in total syntheses of marine alkaloids, aaptamines. Heterocycles. 1999; 50:543–559.
9. Kelly TR, Maguire MP. A synthesis of aaptamine. Tetrahedron. 1985; 41:3033–3036.
10. Pelletier JC, Cava MP. Synthesis of aaptamine, a novel marine alkaloid. Tetrahedron Lett. 1985; 26:1259–1260.
11. Andrew RG, Raphael RA. A new total synthesis of aaptamine. Tetrahedron. 1987; 43:4803–4816.
12. Hibino S, Sugino E, Choshi T, Sato K. Total synthesis of aaptamine with potent a-blocking activity via thermal cyclization of 1-azahexatriene systems. J Chem Soc, Perkin Trans. 1988; 1:2429–2432.

13. Sakamoto T, Miura N, Kondo Y, Yamanaka H. Condensed heteroaromatic ring systems. IX. Total synthesis of aaptamine. Chem Pharm Bull. 1986; 34:2760–2765.
14. Balczewski P, Mallon MKJ, Street JD, Joule JA. A synthesis of aaptamine from 6,7-dimethoxy-1-methylisoquinoline. Tetrahedron Lett. 1990; 31:569–572.
15. Bassoli A, Maddinelli G, Rindone B, Tollari S, Chioccara F. A simple synthesis of aaptamine, a 1H-benzo[de]-1,6-naphthyridine alkaloid. J. of Chem Soc, Chem Commun. 1987; 1987:150–151.
16. von Nussbaum F, Schumann S, Steglich W. Alkaloids from marine organisms. Part 7: Synthesis of bisdemethylaaptamine and bisdemethyloxyaaptamine-a biomimetic approach to the aaptamines?. Tetrahedron. 2001; 57:2331–2335.
17. Gochfeld DJ, El Sayed KA, Yousaf M, Hu JF, Bartyzel P, Dunbar DC, et al. Marine natural products as lead anti-HIV agents. Mini-Rev Med Chem. 2003; 3:401–424. [PubMed: 12769693]
18. Shen YC, Lin TT, Sheu JH, Duh CY. Structures and cytotoxicity relationship of isoaaptamine and aaptamine derivatives. J Nat Prod. 1999; 62:1264–1267. [PubMed: 10514310]
19. Takamatsu S, Hodges TW, Rajbhandari I, Gerwick WH, Hamann MT, Nagle DG. Marine natural products as novel antioxidant prototypes. J Nat Prod. 2003; 66:605–608. [PubMed: 12762791]
20. Sova VV, Fedoreev SA. Metabolites from sponges: inhibitors of β-1,3-glucanase. Chem Nat Comp. 1990; 26:420–422.
21. Ioffina DI, Volkovitskaya OE, Gorkin VZ, Rebachuk NM, Utkina NK, Fedoreev SA. Aaptamine, a new selective type A monoamine oxidase inhibitor. Khimiko-Farmatsevticheskii Zhurnal. 1990; 24:15–16.
22. Evans BE, Rittle KE, Bock MG, DiPardo RM, Freidinger RM, Whitter WL, Lundell GF, et al. Methods for drug discovery: development of potent, selective, orally effective cholecystokinin antagonists. J Med Chem. 1988; 31:2235–2246. [PubMed: 2848124]
23. Hurley LH. DNA and its associated processes as targets for cancer therapy. Nat Rev Can. 2002; 2:188–200.
24. Hutchins RA, Crenshaw JM, Graves DE, Denny WA. Influence of substituent modifications on DNA binding energetics of acridine-based anticancer agents. Biochem. 2003; 42:13754–13761. [PubMed: 14622022]
25. Pettit GR, Hoffmann H, Herald DL, Blumberg PM, Hamel E, Schmidt JM, Chang Y, et al. Antineoplastic agents. 499. Synthesis of hystatin 2 and related 1H-benzo[de][1,6]naphthyridinium salts from aaptamine. J Med Chem. 2004; 47:1775–1782. [PubMed: 15027869]
26. Pettit GR, Hoffmann H, Herald DL, McNulty J, Murphy A, Higgs KC, Hamel E, et al. Antineoplastic agents 491. Synthetic conversion of aaptamine to isoaaptamine, 9-demethylaaptamine, and 4-methylaaptamine. J Org Chem. 2004; 69:2251–2256. [PubMed: 15049616]
27. Gul W, Hammond NL, Yousaf M, Bowling JJ, Schinazi RF, Wirtz SS, de Castro AG, et al. Modification at the C9 position of the marine natural product isoaaptamine and the impact on HIV-1, mycobacterial, and tumor cell activity. Bioorg Med Chem. 2006; 14:8495–8505. [PubMed: 17045480]
28. Valeriote F, Grieshaber CK, Media J, Pietraszkewicz H, Hoffmann J, Pan M, McLaughlin S, et al. Discovery and development of anticancer agents from plants. J Exp Therap and Oncol. 2002; 2:228–236. [PubMed: 12416027]
29. Herlt A, Mander L, Rombang W, Rumampuk R, Soemitro S, Steglich W, Tarigan P, et al. Alkaloids from marine organisms. Part 8: Isolation of bisdemethylaaptamine and bisdemethylaaptamine-9-O-sulfate from an Indonesian *Aaptos* sp. marine sponge. Tetrahedron. 2004; 60:6101–6104.
30. Qu X, Chaires J. Analysis of Drug-DNA Binding Data. Methods Enzymol. 2000; 321:353–369. [PubMed: 10909066]
31. Newman DJ, Cragg GM. Natural Products as Sources of New Drugs over the Last 25 Years. J Nat Prod. 2007; 70:461–477. [PubMed: 17309302]
32. Rees DC, Congreve M, Murray CW, Carr R. Fragment-based lead discovery. Nat Rev Drug Disc. 2004; 3:660–672.
33. Kelly-Borges M, Bergquist PR. A redsescritption of *Aaptaos aaptos* with descriptions of new species of *Aaptos* (Hadromerida: Suberitidae) from New Zealand. J Zool (Lond). 1994; 234:301–323.

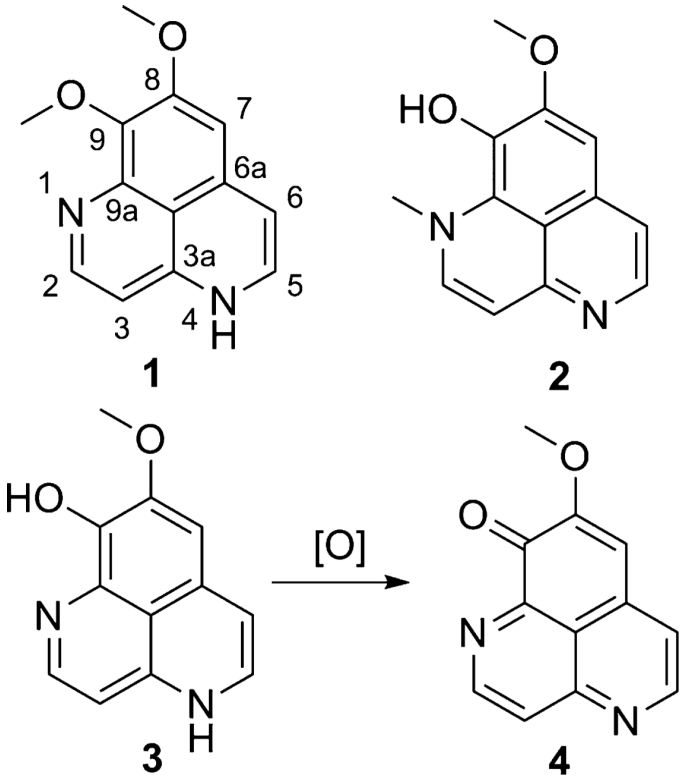

Figure 1.
Structures of major aaptamine related marine natural products.

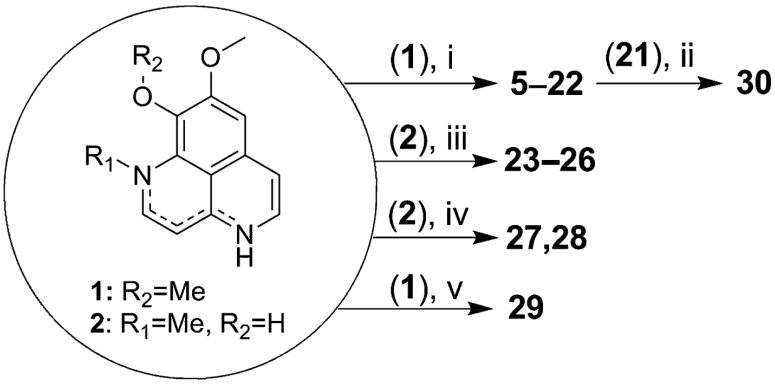

Scheme 1.

Synthetic routes for aaptamine derivatives.[a]

[a](i) RI, KH, DMF, 0 °C; (ii) HBr, 115 °C; (iii) $RS(O)_2Cl$, Et_3N, DCM, 0 °C; (iv) RI_2, Cs_2CO_3, MeC(O), Reflux; (v) BBr_3, DCM, 0 °C.]

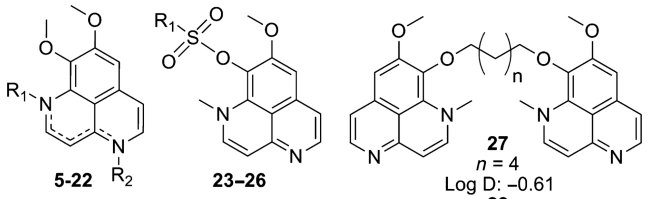

Cpd.	Log D	R_1	R_2
5	2.21	methyl	
6	1.62		methyl
7	1.97	ethyl	
8	2.56		ethyl
9	2.44	propyl	
10	3.03		propyl
11	2.84	butyl	
12	3.42		butyl
13	3.17	3-MeBu	
14	3.75		3-MeBu
15	4.21		hexyl
16	4.03	heptyl	
17	4.61		heptyl
18	4.82	nonanyl	
19	5.40		nonanyl
20	6.01	dodecyl	
21	7.09	dodecyl	dodecyl
22	8.18		hexadecyl
23	1.10	methyl	
24	2.03	propyl	
25	4.01	octyl	
26	3.00	benzyl	

Figure 2.

Four groups of aaptamine derivatives produced through semi-synthesis along with their calculated Log D values at pH 7.4.

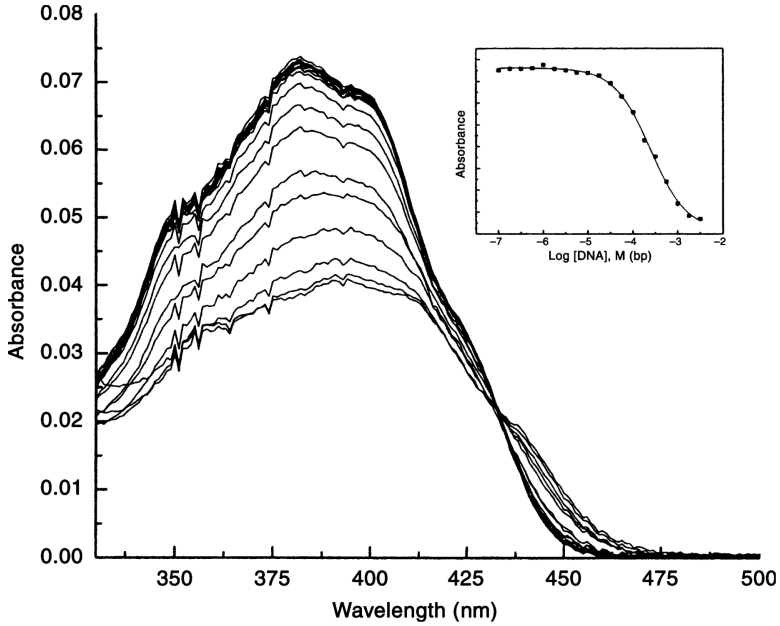

Figure 3.

Aaptamine was evaluated for its ability to bind DNA by UV-vis spectrophotometry. The figure shows the shift in absorbance of a fixed concentration of aaptamine as the DNA concentration is increased. The inset shows the absorbance at 381 nm as a function of log [DNA].

Table 1

Summary of reported relative structure activity relationships for aaptamine based on general improvements of either potency or selectivity

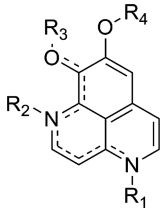

		Effect Relative To Aaptamine (1)		
Position	**Description**	**Cytotoxicity**	**Antiviral**	**Antimicrobial**
R_1	*N*-methylation	0	ND	0
	N-benzylation	+	ND	0
R_1 and R_2	*N,N*-dibenzylation	++	ND	0
R_2	(**2**) *N*-methyl	+	+	0
R_3	ester and phosphate prodrugs	–	–	–
	(**2**) and (**3**) hydroxyl	+	+	0
	(**4**) carbonyl	++	ND	0
R_3 and R_4	demethylation	+	ND	0

(ND) no data, (++) significant improvement, (+) moderate improvement, (0) no significant change, (–) significant decrease.

Table 2

In vitro activity of aaptamine and derivatives (**1, 2, 5-30**) against microbial and AIDS related opportunistic infections

	Antimicrobial (IC_{50}, μM)[a,b]							
Compound	***Ca***	***Cn***	***Cg***	***Ck***	***Sa***	**MR*Sa***	***Mi***	***Af***
1	NA	NA	NA	NA	NR	NA	NA	NA
2	NA	NA	NA	NA	NR	NA	NA	NA
5-15	NA	NA	NA	NA	NR	NA	NA	NA
16	30.6	13.8	NR	NR	13.8	15.3	6.1	61.1
17	NA	45.8	NR	NR	30.6	30.6	30.6	NA
18	18.3	2.8	42.2	14.1	NR	2.8	1.5	11.3
19	28.1	8.4	19.7	11.3	NR	8.4	7.0	42.2
20	NA	1.8	NR	NR	2.0	1.8	0.8	50.3
21	17.7	NA	15	11.5	NR	26.5	NA	NA
22	6.6	3.3	3.3	7.7	NR	3.3	0.6	9.9
23	NA	NA	NA	NA	NR	22.9	NA	NA
24	NA	NA	NA	NA	NR	26.9	NA	NA
25	NA	NA	23.5	NA	NR	NA	NA	NA
26	NA	NA	NA	NA	NR	NA	NA	NA
27	18.6	NA	NA	27.8	NR	18.6	18.6	NA
28	5.6	NA	6.9	5.6	NR	24.1	4.0	24.1
29	NA	NA	NR	NR	NA	NA	NA	NA
30	NA	NA	NA	NA	NR	NA	NA	NA

[a] Control: Amphotericin B IC_{50} = 2.2 μM; NA= Not Active (IC_{50} above 35.4 μM); NR = No Results (Assay discontinued).

[b] Microorganisms: *Ca, Candida albicans; Cn, Cryptococcus neoformans; Cg, Candida glabrata; Ck, Candida krusei; Sa, Stapylococcus aureus*;MR*Sa,* Methicillin Resistant *Staphylococcus aureus; Mi, Mycobacterium intracellulare; Af, Aspergillus fumigatus.*

Table 3

In vitro activity of aaptamine and derivatives a (**1, 2, 5-30**) against chloroquine sensitive and resistant malarial strains *Plasmodium falciparum* (Pf-D6, Pf-W2) and *Mycobacterium tuberculosis* (*Mtb*)

Compound	Anti-malarial (IC_{50}, μM)[a,c]		Mtb MIC (μM)[b,c]
	Pf-D6	Pf-W2	
1	NA	NA	NA
2	5.3	NA	NA
5	8.2	11.9	NA
6, 7	NA	NA	NA
8	3.1	8.6	NA
9	7.4	7.4	NA
10-12	NA	NA	NA
13	13.4	NA	NA
14	11.4	NA	NA
15	2.3	2.3	NA
16	0.6	0.9	4.1
17	2.3	2.9	15.2
18	2.4	2.5	9.8
19	1.9	2.7	6.8
20	1.2	2.0	6.8
21	2.5	3.9	5.1
22	NA	NA	28.9
23	8.2	NA	–
24	5.4	5.4	NA
25	6.2	6.9	–
26	NA	NA	16.1
27	0.4	0.5	NA
28	0.4	0.5	11.2
29	NA	NA	–
30	0.6	0.2	–

[a] Anti-malarial control IC_{50}: (artemesinin) 0.1 and 0.05 μM respectively.

[b] Anti-Mtb control IC_{50}: (rifampin) 0.1 μM.

[c] NA= >8.4 μM; Mtb NA= >47.8 μM; NR = Not active in primary screening

Table 4

In vitro activity of aaptamine and derivatives (**1, 2, 5-30**) against HIV-1 in Human PBM cells with host cytotoxicity (PBM). For some compounds, endpoints were not pursued if cytotoxicity was high

Compound	HIV-1 EC_{50} (μM)[a,b]	Cytotoxicity (IC_{50}, μM)[a,b]		
		PBM	CEM	Vero
1	8.9	<1.0	3.3	23.1
2	7.7	1.1	1.4	2.1
5	NA	21.2	NC	NC
6	39.0	31.6	60.3	58.4
7	35.6	11.7	69.0	46.8
8	NA	95.7	NC	NC
9	4.0	4.3	7.6	74.3
10	24.2	1.4	23.8	NC
11	NA	3.2	5.3	11.8
12	36.7	13.7	5.7	NC
13	31.6	2.6	16.3	17.6
14	31.6	2.3	10.9	17.2
15	NA	3.2	5.3	11.8
16	7.4	2.2	3.8	3.7
17	22.4	1.1	3.5	3.9
18	48.4	1.4	1.2	2.1
19	NA	3.2	<1.0	7.1
20	3.02	<1.0	<1.0	<1.0
21	NA	<1.0	<1.0	<1.0
22	<1.0	1.5	1.8	2.2
23	4.2	1.8	7.3	3.5
24	6.2	1.0	6.0	9.0
25	3.6	2.3	1.3	13.4
26	8.1	10.4	2.0	27.3
27	0.54	<1.0	<1.0	1.2
28	0.52	1.1	<1.0	1.3
29	67.1	NC	NC	NC
30	2.8	3.3	3.8	9.1

[a] HIV-1 EC_{50} Control (AZT) = 0.0048 μM (NC).

[b] NA/NC = Not Active/Cytotoxic at >100 μM.

Table 5

Cytotoxicity of aaptamine (**1**), isoaaptamine (**2**) and selected derivatives (**5-12,14-18,20-28,30**) against leukemia, solid tumor and normal cells in the disk diffusion soft-agar colony formation assay. Activities in bold print represent selectivity. Zones of growth inhibition are displayed in zone units from the disk edge in which 6.5 mm is arbitrarily designated as 200 zone units. Zones greater than 750 units are retested at 4-fold dilutions

		Mouse			Human		
Cpd.	**Dilution Factor**	**Leukemia L1210**	**Colon 38**	**Normal CFU-GM**	**Colon H-116**	**Lung H-125 M**	**Leukemia CEM**
1	1/4	600	500	850	550	500	600
2	1	500	150	450	500	500	500
5	1	450	450	350	450	400	500
6	1	450	400	350	550	400	450
7	1	500	600	400	400	400	600
8	1	450	450	350	300	200	500
9	1	600	600	500	300	350	500
10	1	300	350	300	50	100	–
11	1/4	**200**	**>1000**	**350**	150	100	–
	1/16	**100**	**450**	**150**	–	–	–
12	1	600	650	500	200	250	–
14	1/4	**300**	**550**	**800**	150	200	–
	1/4	**200**	**700**	**150**	–	–	–
15	1/4	**500**	**800**	**550**	200	250	–
	1/16	**200**	**700**	**350**	–	–	–
16	1/4	**600**	**>1000**	**550**	400	400	500
	1/16	**300**	**800**	**450**	–	–	–
	1/64	**200**	**600**	**400**	–	–	–
17	1/4	**700**	**>1000**	**800**	400	500	500
	1/16	**400**	**800**	**450**	–	–	–
	1/64	**150**	**750**	**350**	–	–	–
18	1	650	600	500	400	400	400
20	1	450	550	450	350	400	400
21	1	450	350	600	300	250	350
22	1	350	350	250	150	150	–
23	1/4	300	400	400	400	250	300
24	1/4	350	200	350	350	250	500
25	1/4	500	200	–	400	350	500
26	1/4	450	400	400	400	300	400
27	1	600	600	550	400	350	300
28	1	600	600	500	500	500	600
30	1	300	300	350	250	200	–